A&A 464, L41–L44 (2007)
DOI: 10.1051/0004-6361:20067009

Astronomy & Astrophysics

Letter to the Editor

Deuterium fractionation in the Horsehead edge⋆

J. Pety[1,2], J. R. Goicoechea[2], P. Hily-Blant[1], M. Gerin[2], and D. Teyssier[3]

[1] IRAM, 300 rue de la Piscine, 38406 Grenoble Cedex, France
e-mail: [pety;hilyblan]@iram.fr
[2] LERMA, UMR 8112, CNRS, Observatoire de Paris and École Normale Supérieure, 24 rue Lhomond, 75231 Paris Cedex 05, France
e-mail: [javier;gerin]@lra.ens.fr
[3] European Space Astronomy Centre, Urb. Villafranca del Castillo, PO Box 50727, Madrid 28080, Spain
e-mail: dteyssier@sciops.esa.int

Received 22 December 2006 / Accepted 22 January 2007

ABSTRACT

Context. Deuterium fractionation is known to enhance the [DCO^+]/[HCO^+] abundance ratio over the D/H $\sim 10^{-5}$ elemental ratio in the cold and dense gas typically found in pre-stellar cores.
Aims. We report the first detection and mapping of very bright DCO^+ $J = 3-2$ and $J = 2-1$ lines (3 and 4 K respectively) towards the Horsehead photodissociation region (PDR) observed with the IRAM-30 m telescope. The DCO^+ emission peaks close to the illuminated warm edge of the nebula (<50″ or ∼0.1 pc away).
Methods. Detailed nonlocal, non-LTE excitation and radiative transfer analyses have been used to determine the prevailing physical conditions and to estimate the DCO^+ and $H^{13}CO^+$ abundances from their line intensities.
Results. A large [DCO^+]/[HCO^+] abundance ratio (≥0.02) is inferred at the DCO^+ emission peak, a condensation shielded from the illuminating far-UV radiation field where the gas must be cold (10–20 K) and dense ($\geq 2 \times 10^5$ cm^{-3}). DCO^+ is not detected in the warmer photodissociation front, implying a lower [DCO^+]/[HCO^+] ratio ($<10^{-3}$).
Conclusions. According to our gas phase chemical predictions, such a high deuterium fractionation of HCO^+ can only be explained if the gas temperature is below 20 K, in good agreement with DCO^+ excitation calculations.

Key words. ISM: clouds – ISM: molecules – ISM: individual objects: Horsehead nebula – radio lines: ISM

Molecules are enriched in deuterium over the elemental D/H abundance ($1-2 \times 10^{-5}$, Linsky et al. 2006) in many different astrophysical environments. These include cold, dense cores (Guelin et al. 1982), mid-planes of circumstellar disks (van Dishoeck et al. 2003; Guilloteau et al. 2006), hot molecular cores (Hatchell et al. 1998), and even PDRs (Leurini et al. 2006). Multiply deuterated species were first detected several years ago, e.g. D_2CO in warm gas (Turner 1990) and NHD_2 in cold gas (Roueff et al. 2000). Solomon & Woolf (1973) and Watson (1974) first proposed that deuterium fractionation is mostly caused by gas-phase ion-molecule reactions. Smith et al. (1982) and Roberts & Millar (2000a) confirmed that the deuteration of H_3^+ at low temperatures (<25 K) and of CH_3^+ at higher temperatures (up to ∼70 K) are important precursor reactions in the subsequent deuteration of other species. Roberts & Millar (2000b), Walmsley et al. (2004) and Flower et al. (2006) succeeded in reproducing the amount of several multiply deuterated molecules in cold gas by adding to pure gas-phase chemistry the accretion (freeze-out) of gas-phase molecules onto the surfaces of dust grains. Finally the observed deuterium fractionation in hot cores is thought to result from the liberation of deuterated molecules, trapped in ice mantles in the prestellar phase.

Although it has been studied thoroughly for 30 years, deuterium chemistry is not yet fully understood. With many chemical and physical processes competing for efficient fractionation, models are easier to compare with observations for sources with well described physical conditions. In this letter, we report the detection of very bright DCO^+ lines in the Horsehead edge. In particular, the mane of the Horsehead nebula is a PDR viewed nearly edge-on (inclination <5°) illuminated by the O9.5V star σOri (Abergel et al. 2003; Philipp et al. 2006). Habart et al. (2005) showed that the PDR has a very steep gradient, rising to $n_{\rm H} \sim 2 \times 10^5$ cm^{-3} in less than 10″ or 0.02 pc, at a roughly constant thermal pressure of $\sim 4 \times 10^6$ K cm^{-3}. The newly detected DCO^+ lines arise from a condensation adjacent to the PDR, first detected by Hily-Blant et al. (2005). According to its submillimeter continuum emission, this core (B33-SMM1) is 0.13×0.31 pc long and has an average H_2 density of $\sim 10^4$ cm^{-3} and a peak density of $\sim 6 \times 10^5$ cm^{-3} (Ward-Thompson et al. 2006).

1. Observations and data reduction

The DCO^+ $J = 3-2$ line was observed during 2 h of excellent winter weather (∼0.7 mm of water vapor) using the first polarization (i.e. nine of the eighteen available pixels) of the IRAM-30 m/HERA single sideband multi-beam receiver. We used the frequency-switched, on-the-fly observing mode. We observed along and perpendicular to the direction of the exciting star in zigzags (i.e. ± the lambda and beta scanning direction). The multi-beam system was rotated by 9.6° with respect to the

⋆ Based on observations obtained with the IRAM Plateau de Bure interferometer and 30 m telescope. IRAM is supported by INSU/CNRS (France), MPG (Germany), and IGN (Spain).

Table 1. Observation parameters. The projection center of all the data is $\alpha_{2000} = 05^h40^m54.27^s$, $\delta_{2000} = -02°28'00''$.

Molecule	Transition	Frequency GHz	Instrument	# Pix.[a]	$F_{\rm eff}$[a]	$B_{\rm eff}$[a]	Resol. arcsec	Resol. km s^{-1}	Int. Time[a,b] hours	Noise[c] K	Obs. date[a]
$H^{13}CO^+$	$J = 3-2$	260.255339	30 m/HERA	9	0.90	0.46	13.5″	0.20	5.9/11.3	0.06	Mar. 2006
$H^{13}CO^+$	$J = 1-0$	86.754288	30 m+PdBI	2	0.95	0.78	6.7″	0.20	2.6/4.5	0.10	Sep. 2006
DCO^+	$J = 3-2$	216.112582	30 m/HERA	9	0.90	0.52	11.4″	0.11	1.5/2.0	0.10	Mar. 2006
DCO^+	$J = 2-1$	144.077289	30 m/CD150	2	0.93	0.69	18.0″	0.08	5.9/8.7	0.18	Sep. 2006
$C^{18}O$	$J = 2-1$	219.560319	30 m/HERA	9	0.91	0.55	11.2″	0.11	–	0.26	May 2003
Continuum at 1.2 mm			30 m/MAMBO	117	–	–	11.7″	–	–	–	–

[a] Those columns apply to the 30 m data but not to the PdBI data for the $H^{13}CO^+$ $J = 1-0$ line. [b] Two values are given for the integration time: the on-source time and the telescope time. [c] Noise values estimated at the position of the DCO^+ peak.

scanning direction. This ensured Nyquist sampling between the rows except at the edges of the map. The DCO^+ $J = 2-1$ was observed during 11.3 h using the C150 and D150 single-side band receivers of the IRAM-30 m under ~8.5 mm of water vapor. We used the frequency-switched, on-the-fly observing mode over a 160″ × 170″ portion of the sky. Scanned lines and rows were separated by 8″ ensuring Nyquist sampling. A detailed description of the $C^{18}O$ $J = 2-1$ and 1.2 mm continuum observations and data reductions can be found in Hily-Blant et al. (2005). We estimate the absolute position accuracy to be 3″.

We also use a small part of the $H^{13}CO^+$ ($J = 1-0$ and $J = 3-2$) data, which were obtained with the IRAM PdBI and 30 m telescopes. The whole data set will be comprehensively described in a forthcoming paper studying the fractional ionization across the Horsehead edge (Hily-Blant et al. 2007, in prep.). In short, the $H^{13}CO^+$ $J = 3-2$ line was observed under averaged winter weather (~3.5 mm of water vapor) in rasters along the direction of the exciting star using the first polarization of the unrotated HERA. Each pointing of the rasters was observed in frequency-switched mode. This resulted in a 140″ × 75″ map, Nyquist sampled along the direction of the exciting star but slightly undersampled in the orthogonal direction (i.e. rows separated by 6″ instead of 4.75″). The noise increases quickly at the map edges which were seen only by a fraction of the HERA pixels. We finally used a frequency-switched, on-the-fly map of the $H^{13}CO^+$ $J = 1-0$ line, obtained at the IRAM-30 m using the A100 and B100 3 mm receivers (~7 mm of water vapor) to produce the short-spacings needed to complement a 7-field mosaic acquired with the 6 PdBI antennae in the CD configuration (baseline lengths from 24 to 176 m).

The data processing was done with the GILDAS[1] softwares (Pety 2005). The IRAM-30 m data were first calibrated to the T_A^* scale using the chopper wheel method (Penzias & Burrus 1973), and finally converted to main beam temperatures ($T_{\rm mb}$) using the forward and main beam efficiencies ($F_{\rm eff}$ and $B_{\rm eff}$) displayed in Table 1. The resulting amplitude accuracy is ~10%. Frequency-switched spectra were folded using the standard shift-and-add method, after baseline subtraction. The resulting spectra were finally gridded through convolution by a Gaussian.

2. Results and discussion

Figure 1 presents the DCO^+ $J = 2-1$ and $J = 3-2$ and the $C^{18}O$ $J = 2-1$ integrated intensity maps, together with 1.2 mm continuum emission. All maps are presented in a coordinate system adapted to the source geometry, as described in the figure caption. The DCO^+ emission is concentrated in a narrow, arc-like structure, delineating the left edge of the dust continuum emission. A second maximum is found at the extreme left of the map, associated with a smaller dust continuum peak. Figure 2 shows the $H^{13}CO^+$ and DCO^+ spectra in a cut along the direction of the exciting star at $\delta y = 15''$ (horizontal dashed line of Fig. 1). This cut intersects the DCO^+ emission peak which is close to the illuminated edge of the nebula (<50″ or ~0.1 pc). To our knowledge, this is the brightest DCO^+ emission (4 K) detected in an interstellar cloud close to a bright H_2/PAH emitting region (Habart et al. 2005; Pety et al. 2005). The 15″ spatial shift between the DCO^+ and $C^{18}O$/continuum emission peaks likely results from the steep thermal gradient. The region where the DCO^+ emission is produced, is probably cooler than the region where the $C^{18}O$ lines and 1.2 mm continuum emission peak, i.e. cooler than 30 K, the minimum temperature needed to explain the intensity of the $C^{18}O$ $J = 2-1$ lines in the cloud edge (Goicoechea et al. 2006).

In order to constrain the $[DCO^+]/[HCO^+]$ abundance[2] ratio from the observed line emission, we assumed that both species

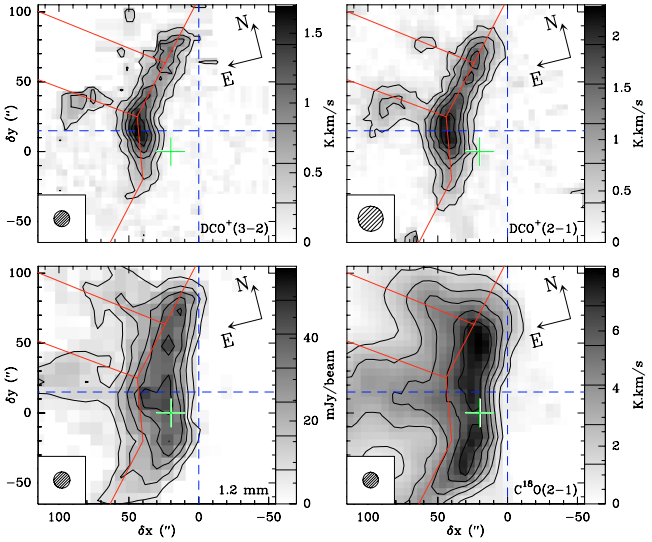

Fig. 1. IRAM-30 m integrated intensity maps. Maps have been rotated by 14° counter-clockwise around the projection center, shown as the green cross at $(\delta x, \delta y) = (20'', 0'')$, to bring the exciting star direction in the horizontal direction and the horizontal zero has been set at the PDR edge, delineated by the dashed blue vertical line. The spatial resolution is plotted in the bottom left corner. Values of contour levels are shown on each image lookup table. The emission of all lines is integrated between 10.1 and 11.1 km s^{-1}.

[1] See http://www.iram.fr/IRAMFR/GILDAS for more information about the GILDAS softwares.

[2] $[DCO^+] = n(DCO^+)/n(H_2)$.

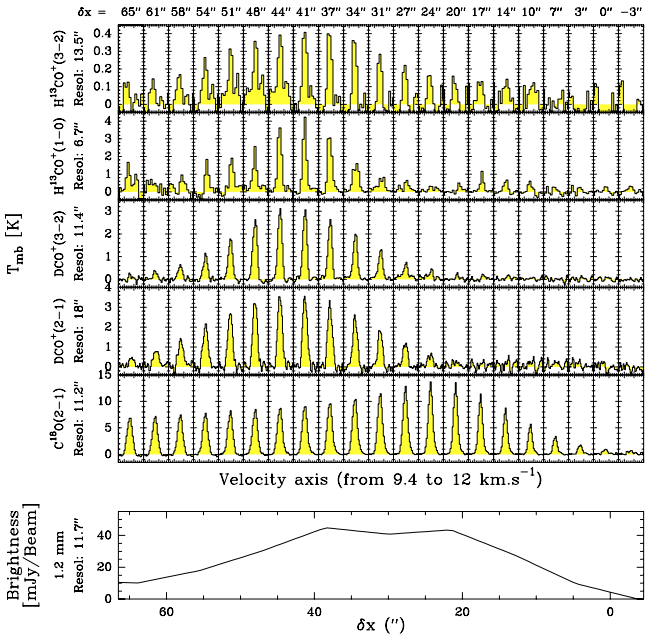

Fig. 2. Cut along the direction of the exciting star at $\delta y = 15''$.

coexist within the same gas (implying the same physical conditions). This assumption is mainly justified by the spatial coincidence of the $H^{13}CO^+$ and DCO^+ emission *peaks* (i.e. where $T_{\rm mb}\{DCO^+(2-1)\}/T_{\rm mb}\left\{H^{13}CO^+(1-0)\right\} \simeq 1$). Besides, we used the $H^{13}CO^+$ lines to determine the line-of-sight HCO^+ column density. Indeed, the direct determination of the HCO^+ column density from its rotational line emission is hampered by the large HCO^+ line opacities and their propensity to suffer from self-absorption and line scattering effects (Cernicharo & Guelin 1987). In addition, large critical densities for HCO^+ (and its isotopologues) are expected even for the lowest-J transitions due to its high dipole moment: ∼4 D (Table 2). Hence, thermalization will only occur at very high densities. For lower densities, $n < n_{\rm crit}$, subthermal excitation dominates as J increases. Therefore, in order to accurately determine the mean physical conditions and the $[DCO^+]/[H^{13}CO^+]$ ratio at the DCO^+ peak, we have used a nonlocal, non-LTE radiative transfer code including line trapping, collisional excitation and radiative excitation by cosmic background photons (Goicoechea 2003; Goicoechea et al. 2006). Collisional rates of $H^{13}CO^+$ and DCO^+ with H_2 and He have been derived from the HCO^+–H_2 rates of Flower (1999).

Assuming a maximum extinction depth of $A_{\rm V} \simeq 50$ along the line-of-sight where DCO^+ peaks (Ward-Thompson et al. 2006), the observed DCO^+ $J = 2-1$ and $J = 3-2$ line intensities are well reproduced (with line opacities ∼1.5) only if the gas is cold (10−20 K) and dense ($n(H_2) \geq 2 \times 10^5$ cm^{-3}). This high density is consistent with the one required to reproduce the CS $J = 5-4$ excitation (Goicoechea et al. 2006) and with the value derived from dust submm continuum emission (Ward-Thompson et al. 2006). The weakness of the $H^{13}CO^+$ $J = 3-2$ line compared to the DCO^+ $J = 3-2$ line is caused in part by its larger Einstein coefficient (a factor ∼1.7 larger) and its higher energy level (see Table 2). This implies that the $H^{13}CO^+$ $J = 3-2$ line is *more* subthermally excited than the analogous DCO^+ line for the derived densities and temperatures. Note that we have not included collisions with electrons in this excitation analysis. In fact, the expected ionization fraction in such a cold and dense

Table 2. Einstein coefficients, upper level energies and critical densities for the range of temperatures considered in this work.

Molecule	Transition	A_{ij} (s^{-1})	$E_{\rm up}$ (K)	$n_{\rm crit}$ (cm^{-3})
$H^{13}CO^+$	$J = 1-0$	3.9×10^{-5}	4.2	$\sim 2 \times 10^5$
$H^{13}CO^+$	$J = 3-2$	1.3×10^{-3}	25.0	$\sim 3 \times 10^6$
DCO^+	$J = 2-1$	2.1×10^{-4}	10.4	$\sim 6 \times 10^5$
DCO^+	$J = 3-2$	7.7×10^{-4}	20.7	$\sim 2 \times 10^6$

condensation is usually low, $<10^{-7}$ (Caselli et al. 1999). The derived DCO^+ and $H^{13}CO^+$ column densities toward the DCO^+ peak are $\simeq (0.5-1) \times 10^{13}$ cm^{-2} (i.e., $[DCO^+] \simeq [H^{13}CO^+] \simeq (1-2) \times 10^{-10}$). Assuming a $^{12}C/^{13}C = 60$ isotopic ratio (Milam et al. 2005), we finally find a $[DCO^+]/[HCO^+] \geq 0.02$ abundance ratio.

In order to understand the observed deuterium fractionation in the dense gas close to the Horsehead PDR, we have modeled the steady state deuterium gas phase chemistry in a cloud with a proton density $n_{\rm H} = n({\rm H}) + 2n(H_2) = 4 \times 10^5$ cm^{-3} illuminated by a far-UV field 60 times the mean interstellar radiation field. We used the `Meudon PDR code`[3], a photochemical model of a unidimensional PDR (see Le Bourlot et al. 1993; Le Petit et al. 2006, for a detailed description) and its associated chemical reaction network. As this network only includes singly deuterated species, we added the D_2 and HD_2^+ species and associated reactions from Flower et al. (2006). Nevertheless, these additional reactions do not affect much the predicted DCO^+ abundances. Only H_2, HD and D_2 form on grain surfaces because the used chemical network allows only H and D atoms to accrete onto dust grains. We chose the following gas phase abundances: D/H = 1.6×10^{-5}, He/H = 0.1, O/H = 3×10^{-4}, C/H = 1.4×10^{-4}, N/H = 8×10^{-5}, N/H = 8×10^{-5}, S/H = 3.5×10^{-6} (Goicoechea et al. 2006), Si/H = 1.7×10^{-8}, Na/H = 2.3×10^{-9} and Fe/H = 1.7×10^{-9}.

We first investigated the role of gas thermodynamics in the HCO^+ deuterium fractionation. To do this, we stopped to solve the thermal balance when the far-UV absorption was large enough so that the temperature reaches a minimum value that we kept constant in the most shielded regions of the PDR. Figure 3 shows the predicted temperature profiles as well as the $[H_2D^+]/[H_3^+]$ and $[DCO^+]/[HCO^+]$ abundance ratios as a function of the cloud depth for a minimum value of $T_{\rm k} = 15$, 20, 30 and 60 K. The predicted $[DCO^+]/[HCO^+]$ ratio scales with the $[H_2D^+]/[H_3^+]$ ratio, as expected when DCO^+ gets fractionated by the reaction of CO with H_2D^+ and mainly destroyed by dissociative recombination with electrons (see e.g. Guelin et al. 1982). The displayed models also imply that low gas temperatures (≤20 K) are needed to reproduce the observed $[DCO^+]/[HCO^+]$ ratio at $\delta x = 40-45''$ ($A_{\rm V} \sim 10-20$ depending on the assumed density profile). This is easily understood because the exchange reaction between H_3^+ and HD is most efficient at low temperatures (Gerlich et al. 2002). Therefore, the observed $[DCO^+]/[HCO^+] \geq 0.02$ abundance ratio can be reproduced using gas phase chemistry only if the gas cools down from the photodissociation front to ≤20 K, in good agreement with the DCO^+ excitation calculations. Note, however, that CO freeze-out is believed to further enhance the $[DCO^+]/[HCO^+]$ ratio over the values predicted by pure gas phase fractionation by increasing the abundance of H_3^+ and H_2D^+ (Brown & Millar 1989;

[3] Publicly available at `http://aristote.obspm.fr/MIS/`

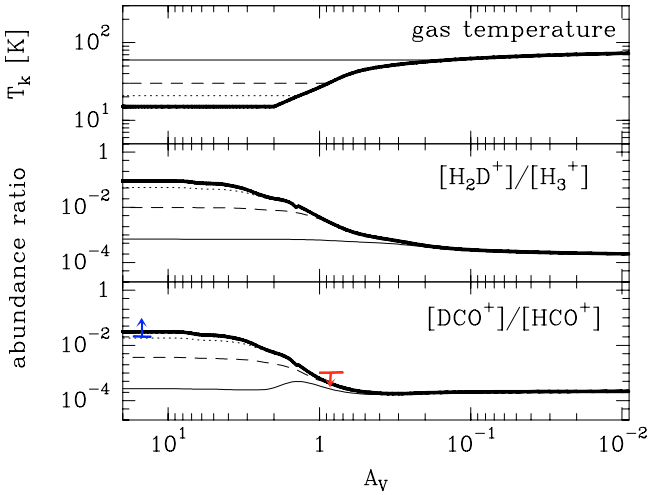

Fig. 3. Chemical models for different minimum gas temperatures: 15, 20, 30 and 60 K. The density is $n_H = 4 \times 10^5$ cm^{-3} and the illuminating radiation field is $\chi = 60$. Temperature profiles and predicted $[H_2D^+]/[H_3^+]$ and $[DCO^+]/[HCO^+]$ abundance ratios are shown as a function of A_V. The $[DCO^+]/[HCO^+]$ ratios inferred from observations in the cold condensation at $\delta x \sim 40-45''$ and in the warm PDR gas at $\delta x \sim 10-15''$ are shown respectively with the blue and red arrows.

Caselli et al. 1999). The $C^{18}O$ $J = 2-1$ emission shown in Fig. 2 substantially decreases at the DCO^+ peak. This behavior is reminiscent of CO depletion but it could also come from a combination of lower excitation and of opacity effects. Future observations of molecular tracers of gas depletion are needed to constrain the dominant scenario.

The DCO^+ lines stay undetected in the warm gas where HCO^+ (not shown here) and $H^{13}CO^+$ still emit. Indeed, DCO^+ can not be abundant in the photodissociation front, where the large photoelectric heating rate implies warm temperatures ($T_k > 50$ K), because the reaction of H_2D^+ with H_2 dominates and implies a low H_2D^+ abundance ($[H_2D^+]/[H_3^+] \simeq 2 \times 10^{-4}$). From the upper limit of the DCO^+ emission at $\delta x = 10-15''$ ($A_V \sim 1$), we estimate a low abundance ratio $[DCO^+]/[HCO^+] < 10^{-3}$ in the far-UV photodominated gas, in agreement with the model predictions.

The small distance to the Horsehead nebula (~400 pc), its low FUV illumination and its high gas density imply that many physical and chemical processes, with typical gradient lengthscales ranging between 1″ and 10″, can be probed in a small field-of-view (less than 50″). The Horsehead edge thus offers the opportunity to study in great detail the transition from the warmest gas, dominated by photodissociation processes and photoelectric heating, to the coldest and shielded gas where strong deuterium fractionation is taking place. Therefore, the Horsehead edge is the kind of source needed to serve as a reference for PDR models (Pety et al. 2006) and offers a realistic template to analyze more complex galactic or extragalactic sources.

Acknowledgements. We thank M. Guelin for useful comments and the IRAM PdBI and 30 m staff for their support during the observations. J.R.G. was supported by an *individual Marie Curie fellowship*, contract MEIF-CT-2005-515340.

References

Abergel, A., Teyssier, D., Bernard, J. P., et al. 2003, A&A, 410, 577
Brown, P. D., & Millar, T. J. 1989, MNRAS, 237, 661
Caselli, P., Walmsley, C. M., Tafalla, M., Dore, L., & Myers, P. C. 1999, ApJ, 523, L165
Cernicharo, J., & Guelin, M. 1987, A&A, 176, 299
Flower, D. R. 1999, MNRAS, 305, 651
Flower, D. R., Pineau Des Forêts, G., & Walmsley, C. M. 2006, A&A, 449, 621
Gerlich, D., Herbst, E., & Roueff, E. 2002, Planet. Space Sci., 50, 1275
Goicoechea, J. R. 2003, Ph.D. Thesis, Universidad Autonoma de Madrid
Goicoechea, J. R., Pety, J., Gerin, M., et al. 2006, A&A, 456, 565
Guelin, M., Langer, W. D., & Wilson, R. W. 1982, A&A, 107, 107
Guilloteau, S., Piétu, V., Dutrey, A., & Guélin, M. 2006, A&A, 448, L5
Habart, E., Abergel, A., Walmsley, C. M., Teyssier, D., & Pety, J. 2005, A&A, 437, 177
Hatchell, J., Millar, T. J., & Rodgers, S. D. 1998, A&A, 332, 695
Hily-Blant, P., Teyssier, D., Philipp, S., & Güsten, R. 2005, A&A, 440, 909
Le Bourlot, J., Pineau Des Forets, G., Roueff, E., & Flower, D. R. 1993, A&A, 267, 233
Le Petit, F., Nehmé, C., Le Bourlot, J., & Roueff, E. 2006, ApJS, 164, 506
Leurini, S., Rolffs, R., Thorwirth, S., et al. 2006, A&A, 454, L47
Linsky, J. L., Draine, B. T., Moos, H. W., et al. 2006, ApJ, 647, 1106
Milam, S. N., Savage, C., Brewster, M. A., Ziurys, L. M., & Wyckoff, S. 2005, ApJ, 634, 1126
Penzias, A. A., & Burrus, C. A. 1973, ARA&A, 11, 51
Pety, J. 2005, in SF2A-2005: Semaine de l'Astrophysique Française, ed. F. Casoli, T. Contini, J. M. Hameury, & L. Pagani, 721
Pety, J., Goicoechea, J. R., Gerin, M., et al. 2006, in SF2A-2006: Semaine de l'Astrophysique Française [arXiv:astro-ph/0612588]
Pety, J., Teyssier, D., Fossé, D., et al. 2005, A&A, 435, 885
Philipp, S. D., Lis, D. C., Güsten, R., et al. 2006, A&A, 454, 213
Roberts, H., & Millar, T. J. 2000a, A&A, 364, 780
Roberts, H., & Millar, T. J. 2000b, A&A, 361, 388
Roueff, E., Tiné, S., Coudert, L. H., et al. 2000, A&A, 354, L63
Smith, D., Adams, N. G., & Alge, E. 1982, ApJ, 263, 123
Solomon, P. M., & Woolf, N. J. 1973, ApJ, 180, L89
Turner, B. E. 1990, ApJ, 362, L29
van Dishoeck, E. F., Thi, W.-F., & van Zadelhoff, G.-J. 2003, A&A, 400, L1
Walmsley, C. M., Flower, D. R., & Pineau des Forêts, G. 2004, A&A, 418, 1035
Ward-Thompson, D., Nutter, D., Bontemps, S., Whitworth, A., & Attwood, R. 2006, MNRAS, 369, 1201
Watson, W. D. 1974, ApJ, 188, 35